



Jacksonville State University  
**JSU Digital Commons**

---

Research, Publications & Creative Work

Faculty Scholarship & Creative Work

---

2010

## **Gadolinium Concentration Analysis in Brain Phantom by X-ray Fluorescence**

Musaed Almalki

Samir Abdul Majid

Philip H. Butler

Lou Reinisch

Follow this and additional works at: [https://digitalcommons.jsu.edu/fac\\_res](https://digitalcommons.jsu.edu/fac_res)



Part of the [Earth Sciences Commons](#)

---

# Gadolinium concentration analysis in brain phantom by X-ray fluorescence

Musaed Almalki · Samir Abdul Majid · Philip H. Butler · Lou Reinisch

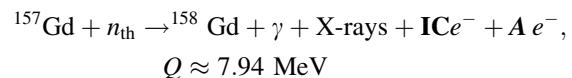
Received: 22 December 2009 / Accepted: 21 June 2010 / Published online: 2 July 2010  
© Australasian College of Physical Scientists and Engineers in Medicine 2010

**Abstract** We have measured the X-ray fluorescence from gadolinium as a function of concentration and position in tumors of different sizes and shapes in a head phantom. The gadolinium fluorescence was excited with a 36 GBq Am-241 source. The fluorescence signal was detected with a CdTe detector and a multi-channel analyzer. The fluorescence peak was clearly separated from the scattered X-rays. Concentrations of 5.62–78.63 mg/ml of Gd ion were used in 1, 2, and 3 cm diameter spherical tumors and a 2 × 4 cm oblate spheroid tumor. The data show trends approaching saturation for the highest concentrations, probably due to reabsorption in the tumor. A comparison of X-ray photographic imaging and densitometer measurements to determine concentration is also presented.

**Keywords** Gadolinium concentration · Brain tumor · Gadolinium · X-ray fluorescence

## Introduction

In recent years gadolinium (Gd) has received attention in research for its application to neutron capture therapy. Gd neutron capture reactions produce Auger electrons, **A**, internal conversion electrons, **IC**, prompt gamma rays,  $\gamma$ , and X-rays.



The Auger electrons and higher energy electrons induce double strand DNA cleavage. The long range gamma rays that are released in the  $^{157}\text{Gd}(n, \gamma)$  reaction can deliver a dose to the healthy tissue, which reduces the localization effect of neutron capture therapy but also increases the probability of striking all the tumor cells [1–4]. Only a small fraction of the dose penetrates the surrounding normal tissue [5–8]. If neutron capture by Gd is going to be used, it is important to assess the dose delivered to the patient, which means it is important to know the amount of the Gd inside the brain tumor, either before or during exposure to the neutrons [9]. The current magnetic resonance imaging technique (MRI) does not provide adequate information for two reasons. First, the technique is generally qualitative. Second, the imaging takes a long time, during which part of the Gd will have been biologically eliminated. Information on concentration, build-up, or elimination of the Gd from an organ is significant in Gd neutron therapy [10, 11].

There are many possible ways to determine the concentration of the Gd in the tumor. The first method that we investigated was to measure the attenuation of the X-rays by the Gd. The attenuation could be measured with dual image subtraction, subtracting the image before the Gd is

---

M. Almalki · P. H. Butler  
Department of Physics and Astronomy, University of  
Canterbury, Christchurch, New Zealand

M. Almalki  
Ministry of Health, Jeddah, Saudi Arabia

S. A. Majid  
Department of Nuclear Engineering, King Abdulaziz University,  
Jeddah, Saudi Arabia

L. Reinisch (✉)  
Department of Physical and Earth Sciences, Jacksonville State  
University, 700 Pelham Road North, Jacksonville, AL 36265,  
USA  
e-mail: lou.reinisch@att.net

injected, from the image after the Gd is injected. Alternatively, dual energy subtraction could be used where the image from a detector sensitive to X-ray photons with energies less than the k-edge absorption is subtracted from an image created by a detector sensitive to X-ray photons with energies greater than the k-edge of Gd. A simplified method of X-ray absorption is to use an X-ray tube with a potential greater than 70 kV. This would emit X-rays and the majority of the photons would have energies greater than the k-edge of Gd. So, the resulting image is dominated by the Gd absorption. It is this simplified technique using a single X-ray image that we investigated here.

The other technique we used to determine the Gd concentration was to measure the X-ray fluorescence. Here, a monochromatic source of X-rays with an energy above the k-edge of Gd is incident upon the tumor. The scattered X-rays with the characteristic energy of the fluorescence are then counted. We investigate these two different methods of noninvasively measuring Gd concentration in a brain tumor using a head phantom.

## Materials and methods

### Phantom

Variables of the measurement were: tumor size, depth of the tumor, concentration of the Gd solution and tumor geometry. These parameters were measured with a transparent head phantom (Churchin Association, Smithtown, NY, USA). This phantom was supplied with 1, 2, and 3 cm diameter spherical tumor vessels and a  $2 \times 4$  cm oblate spheroid tumor vessel. These vessels, simulating the tumor, could be filled with water and a known concentration of Gd and placed in specific locations in the head phantom.

The head phantom, containing Gd agent in a tumor vessel, was put in front of an Am-241 source. Lateral and vertex positions of the head phantom were taken, with the X-ray detector positioned as shown in Fig. 1. The characteristics X-ray measured was 42.98 keV.

In Fig. 1, we show a drawing of the set up with the source and detector in the lateral position. The position of the tumor in the skull is determined with a laser sight (not shown) allowing us to determine the position of the tumor to better than  $\pm 1.0$  mm. The distance from the inside of the skull to the center of the tumor is the tumor depth. The source is positioned 6 cm from the exterior of the skull. The dashed arrows show the incident and emitted radiation.

### X-ray imaging

To obtain the size and the shape of the tumor by the radiographic method, a general X-ray machine with radiograph

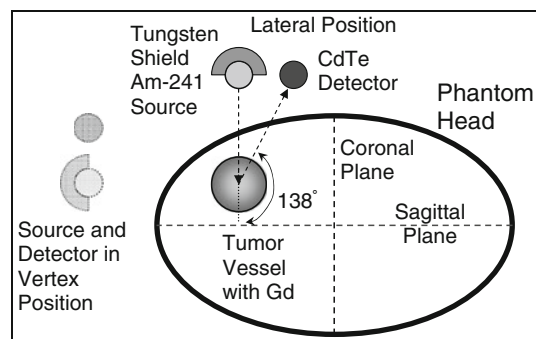


**Fig. 1** The head phantom containing the tumor vessel is shown. The source and detector are in the lateral position. The source and detector are also shown as a lighter image in the vertex position

film was used. The left lateral of the head phantom was put in contact with the table and the median sagittal plane was parallel to the film. The X-ray beam was perpendicular to the film and sagittal plane. The central ray was centered to the right external auditory meatus. Radiographic exposure factors of the experiments were fixed at 73 kVp, 20 mA, with a source film distance of 105 cm. The cassette size was a 24 cm  $\times$  30 cm. The film was developed with standard techniques and the optical density of the film was measured with a Model 07-443 Densitometer (Nuclear Associates, Division of Victoreen Inc, Phoenix, USA). The differences of optical density in the X-rays films were obtained when the densities from the center of the tumor vessels were subtracted from the densities of the darkest point on the X-ray films (outside the image of the head phantom).

### X-ray fluorescence

To measure the X-ray fluorescence, Gd atoms in the tumor vessel were excited by a 36 GBq (0.97 Ci) of Am-241 source ( $T_{1/2} = 432.7$  years). It produced 59.5 keV gamma rays with a relative intensity of 0.357 per disintegration. The emitted characteristic fluorescence radiation was measured by a cadmium telluride (CdTe) detector (Amptek Inc, USA). The XR-100T-CdTe detector had 1.0 mm thick of CdTe and a 100  $\mu$ m thick beryllium window. The position of the detector is beside the Am-241 source, which is mounted on the column of tungsten, at a 138° angle with respect to the axis of the gamma ray beam. The distance from the surface of the head phantom to the Am-241 source was adjusted to be 6.0 cm and the exposure time was chosen to be real time and set for 30 min. The different size and shape of the tumor vessels were selected for exposure. These sizes were spheres with diameters of 1.0, 2.0, and 3.0 cm, and an oblate spheroid with  $2.0 \times 4.0$  cm diameters. The depths of the tumor were measured from the surface of the head phantom to the center of the tumor

vessel. The depths ranged from 0.5 to 5.5 cm between the center of the tumor and interior wall of the skull.

The X-ray photons were digitized on the Genie 2000 PC multichannel analyzer (MCA) (Canberra Company, Meriden, CT, USA). The intensity of the fluorescence peak is obtained by fitting the background to a cubic equation subtracting the background and then integrating the fluorescence. Concentrations from 5.62 to 78.63 mg/ml of Gd ion in the tumor vessel were used in the phantoms. The Gd is a constituent of the commercial contrast agent, Magnevist (Schering AG, Germany).

The total counts of the fluorescence peak was measured as a function of the Gd concentration and as a function of the tumor depth for tumor vessels of the following sizes: 1.0, 2.0, 3.0, and 2.0 × 4.0 cm. For each tumor, two measurements were made: the first for the tumor with the skull filled with water to mimic biologic tissue, the second for one without water. When using the 1.0 cm tumor the total amount of Gd in the tumor was small, and it was difficult to measure the fluorescence X-rays from Gd when the head phantom was filled with water. Therefore, all the experiments for the 1.0 cm tumor were conducted only in the head phantom without water.

Although it is not physiological to not put water into the head phantom, a comparison of the two measurements, with and without water, should indicate only the attenuation of the water. Thus, one can check that the measured counts are reasonable and the measurement geometry is as expected. Since the attenuation of the water in the head phantom should only change with the location of the tumor and not the concentration of Gd in the tumor, we took the measured counts for each position with the head full of water and divided by the measured counts for each position with the head empty. This number is always less than 1.0 and represents the attenuation of the water in the head phantom. The measured attenuation is compared with the expected attenuation of water.

The Gd X-ray fluorescence (XRF) peak is at 42.98 keV. It is important to consider if this peak overlaps any other X-ray peak and might distort the measurements. Materials subject to direct radiation from the source are carbon, nitrogen, oxygen and hydrogen from brain tissue and calcium and phosphorous from the skeletal bones. All these elements have XRF peaks that are far below the Gd XRF peak. The highest energy peak is that of calcium at about 4 keV. Materials that might be subject to secondary radiation are Cd and Te from the CdTe detector itself, W or Pb if any of these elements are used for collimation. Cd and K lines are at about 23 keV, while those of Te are at about 27 keV; both are far from the Gd peak. Moreover, because the secondary radiation intensity is much less than the primary beam, the excitation will be small. Lead or tungsten atoms will not be

excited because their excitation energies are above the 59.5 keV from the Am-241.

### Results

#### X-ray fluorescence

The scattering angle for the setup was determined to be approximately 138°. At 138° the Compton scattering of the incident radiation (59.5 keV) made a broad peak near 49 keV. The  $K_{\alpha}$  characteristic X-ray peak of the Gd atoms (42.98 keV) was clear and easily separated from the scattered photon peak (49 keV) as shown in Fig. 2.

In Fig. 3, we show the measured intensities from the 1 cm diameter tumor in the phantom head without water in the head and measured with the source and detector in the lateral position. The depth of the tumor was 0.5–5.5 cm in

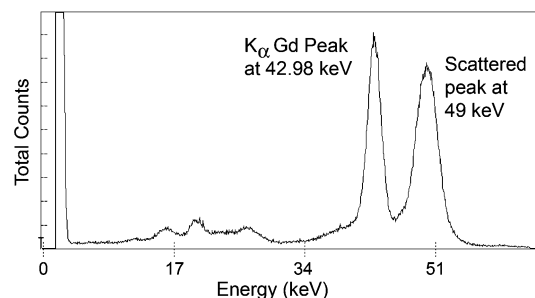


**Fig. 2** Spectrum of the  $K_{\alpha}$  characteristic X-ray of the Gd obtained from a 3 cm diameter tumor vessel, which contained 50.55 mg/ml of Gd at a depth of 1.0 cm and measured in the lateral position

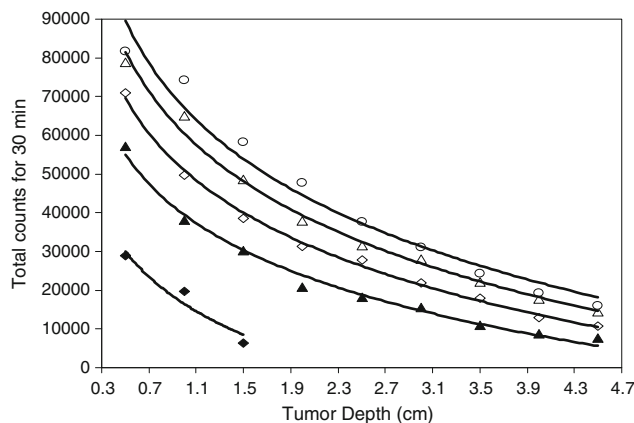


**Fig. 3** Integrated counts of X-ray fluorescence of Gd as a function of the depth in the head phantom for a 1 cm diameter spherical tumor measured in the lateral position. The phantom skull was not filled with water. The filled diamonds are measured with a concentration 15.73 mg/ml of Gd, the filled triangles are with 31.45 mg/ml, the open triangles are with 47.18 mg/ml, the open circles are with 78.63 mg/ml. The lines are drawn to guide the eye

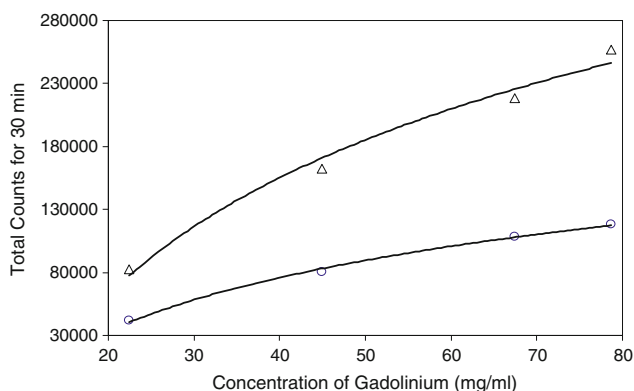


**Fig. 4** Integrated counts of X-ray fluorescence of Gd as a function of the Gd concentration for a 2 cm diameter spherical tumor measured in the lateral position. The tumor is 2.0 cm inside the skull. The *triangles* were measured when the phantom skull was not filled with water. The *circles* were measured when the phantom skull was filled with water. The *lines* are drawn to guide the eye

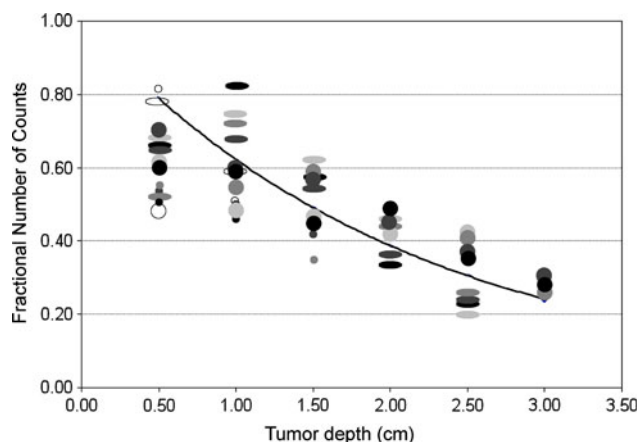
0.5 cm steps. We plot the total counts as a function of the tumor depth, for each Gd concentration. This figure shows that the total counts decreased as the tumor depth increased inside the head phantom, as one would expect.

Figure 4 shows the comparisons of the total counts of the Gd X-ray fluorescence as a function of the Gd concentration for the head phantom with and without water. The measurements were taken at the depth of 2.0 cm for a spherical tumor vessel with a diameter 2.0 cm. The figures show that the total counts increase as the concentration increased and they were higher for the phantom head without water. Similar data were collected at all depths.

The relationship between the measured attenuation of the water in the skull using the different Gd concentrations (mg/ml) and the different tumour depths are shown in Fig. 5. The line is the predicted attenuation for the known scattering and absorption of water. The incident radiation of 59.5 keV from the source and the emitted characteristic X-ray of 42.98 keV undergo attenuation by the water inside the head phantom in the lateral position. The attenuation of the incoming 59.5 keV gamma ray is given by  $\exp[-\mu(59.5 \text{ keV}) x]$ , while the attenuation due to the emitted characteristic X-ray of 42.98 keV is  $\exp[-\mu(42.98 \text{ keV}) x']$ , where  $x$  and  $x'$  are the distance of the incident radiation and emitted characteristic X-ray, respectively, that travel through the water. The correlation between the attenuation of the experimental measured and the calculated attenuation was observed with an  $R^2 = 0.72$ .

#### X-ray imaging

Radiographic images are shown in Fig. 6. In this case the tumor of 3 cm diameter containing the Gd agent, was placed at a 1.5 cm depth inside a head phantom containing



**Fig. 5** Fractional number of counts from tumors measured with water in the head phantom to no water in the head phantom measured at different tumor depths and tumor sizes and concentrations of Gd. The *large dots* are 3 cm tumor sizes, with *black* being 79 mg/ml Gd, *dark gray* is 62 mg/ml Gd, *medium gray* is 51 mg/ml Gd, *light gray* is 28 mg/ml Gd and *white* is 5.6 mg/ml Gd. The *small dots* are 2 cm tumor sizes, with *black* being 79 mg/ml Gd, *dark gray* is 67 mg/ml Gd, *medium gray* is 45 mg/ml Gd, and *white* is 22 mg/ml Gd. The *ovals* are the 2 × 4 cm tumor sizes with *black* being 79 mg/ml Gd, *dark gray* is 58 mg/ml Gd, *medium gray* is 41 mg/ml Gd, *light gray* is 25 mg/ml Gd and *white* is 8.3 mg/ml Gd. The *line* is an exponential fit of water attenuation. The  $R^2$  of the fit = 0.72

water. The radiographic film shows the tumor image with Gd concentrations of 0.56 mg/ml in (A) and 78.63 mg/ml in (B). The presence of the Gd compound in the tumor vessel inside the head phantom was clearly visualized on the radiographic film. The outline of the tumor vessel was apparent. As the concentration of Gd was increased, the clarity of the image of the tumor improved. The differences of optical density in the X-rays films as shown in Fig. 7 were obtained when the densities from the center of the tumor vessels were subtracted from the densities of the darkest point on the X-ray films. This figure shows that the “noise” in the film density was excessive with the lower concentrations of the Gd.

#### Discussion

Magnevist is a well-known agent for magnetic resonance image (MRI) tumor imaging and contains Gd; this element has the highest cross-section for thermal neutrons and shows promise for Gd neutron capture therapy. The maximum Gd concentration was limited by its concentration in the Magnevist, where one milliliter of Magnevist solution contains 469 mg of gadopentetic acid and dimeglumine salt, this corresponds to 78.63 mg of Gd. Throughout this article, we report on the concentration of Gd ion that is present in the tumor.

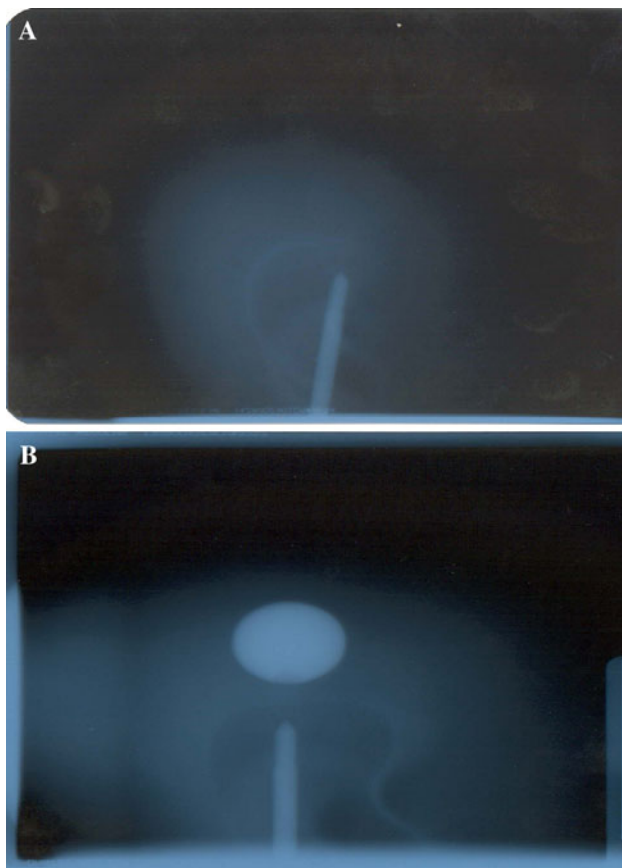


**Fig. 6** Radiograph of the 3 cm tumor vessel 1.5 cm inside the head phantom taken at 73 KVp, 20 mA, and at 105 cm SFD. In **a** the Gd concentration is 0.56 mg/ml, in **b** the Gd concentration is 78.63 mg/ml

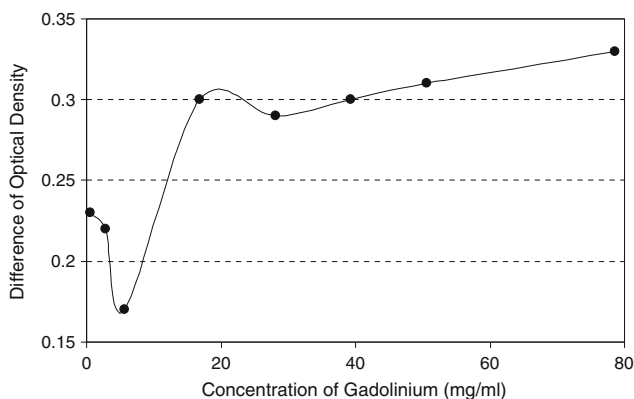


**Fig. 7** Difference of optical density (center of the tumor compared to area immediately adjacent to the tumor) versus concentration of Gd in a 3.0 cm diameter tumor vessel, at 1.5 cm depth inside the head phantom, in the lateral position. The smooth *line* between the data points is drawn to guide the eye

The sizes and the shapes of the tumors in the brain phantom were confirmed by radiographic film of the tumor vessels. These contained different concentrations of Gd

inside the head phantom filled with water as shown in Fig. 6. The radiographic film was taken of a 3.0 cm diameter tumor vessel in the lateral position at 1.5 cm depth with different Gd concentrations such as 0.56 and 78.63 mg/ml. As the Gd in the tumor vessel has a high atomic number and high density, the incident gamma radiation interaction would be increased, leading to increased photon attenuation, which in turn made the tumor vessel appear very bright on the film. Consequently, the greater the concentration of Gd, the clearer the tumor image appeared. However, as shown in Fig. 7, it is not practical to determine the concentration of Gd from the density on the film. Even though a difference in optical density is plotted, partially compensating for film age, strength of the film processing chemicals and other variables, the optical density differences have a significant amount of noise for the lower concentrations.

The minimum value of the Gd concentration for each of the four tumors was limited by the minimum detectable level of fluorescence by the detector. The results show that the total fluorescence counts increased as the concentration of the Gd in the tumor vessel increased, as expected. The relation between the counts and the concentration for each measurement does not follow a straight line (see Fig. 4), possibly due to self absorption of the X-ray emissions inside the tumor vessel. As the Gd concentration increases, a higher fraction of the emitted characteristic X-rays is absorbed within the tumor. This leads to a fluorescence intensity that shows a tendency towards saturation rather than a linear increase.

The other factor impacting on the experimental outcome was the location of the tumor vessel inside the head phantom (i.e. the depth of the tumor as measured from the surface of the skull to the center of the tumor vessel). Measurements showed that at a depth of 2.0 cm for the tumor vessel with a diameter of 1.0 cm and also, at a depth of 2.5 cm for tumors size of 2.0, 3.0, and 2.0 × 4.0 cm with a minimum concentration of Gd (15.73 mg/ml) the fluorescence signal was not separable from the background. Furthermore, it was clear that the deeper the tumor was inside the head phantom, the lower the counts. That was, in part, due to the increased distance from the CdTe detector and from the Am-241 source and owing to the attenuated and absorption of incident as well as emitted characteristic X-ray in the water inside both the tumor and in the head phantom. The tumor was not a point source and, therefore, the counts do not follow exactly the inverse square law.

The effect of water absorption (water is closely equivalent to biological tissue, as effective atomic number of water and tissue are both 7.4) was found when the experiment was repeated without water inside the head phantom. In these results, the counts were lower for the head phantom containing water than those of the empty head phantom under the same condition (i.e. tumor size, tumor depth,

and Gd concentration). The results of the characteristic X-ray, between the head phantom with and without water, are shown in the tumor vessel 2.0 cm diameter at a depth of 2.0 cm and containing 78.63 mg/ml of Gd concentration at the vertex position, where the total count from the head phantom containing water was 149,502 compared with 218,100 counts from the head phantom without water. The total count was reduced by factor 1.5. On the other hand, at a depth of 4.5 cm in the tumor vessel of 3.0 cm diameter, the total count obtained from the head phantom containing water was 63,786 compared with 270,684 counts (reduced by a factor of 4.2) from the empty head phantom. Counts were reduced threefold when an irregular tumor vessel of  $2.0 \times 4.0$  cm, at a depth of 4.0 cm, was used, where counts from the head phantom containing water were 72,068 compared with 217,494 from head phantom without water. Generally, in the same conditions (i.e. tumor size, tumor depth, and Gd concentration) the total counts without water were higher. The only effect that is responsible for the difference in total counts is the presence of water inside the head phantom. This water caused the attenuation of the incident 59.5 keV and the X-ray emitted from the tumor vessel.

Total counts from the three tumor sizes inside the head phantom in the lateral and vertex positions, showed consistency and a tendency for saturation at higher concentration. Total counts obtained from the tumor vessels of 2.0, 3.0 and  $2.0 \times 4.0$  cm at depths of 1.5 and 2.0 cm, respectively, in the head phantom containing water, shows that increasing the tumor vessel size, increases the total counts for the tumor vessel depths. It should be noted that no results were obtained for the 1.0 cm tumor, with water in the head phantom. Also, it can be observed that for the same total amount of Gd, different counts are obtained by using different shapes. The highest counts were obtained from 3.0 cm tumor. The 1.0 cm tumor gave the lowest counts because it contained the least amount of total Gd.

The collection time used for the fluorescence signal detection in this work was 30 min. This is too long for measuring instantaneous concentration. On the other hand, the source activity used was 0.97 Ci ( $3.6 \times 10^{10}$  Bq). In order to reduce counting time, source activity could be increased. Source activity of about 100 Ci ( $3.7 \times 10^{12}$  Bq) is practical and can reduce collection time to about 0.3 min (18 s). Reduction of time can also be achieved by using a higher efficiency detector. Our detector of CdTe had about  $1 \text{ cm}^2$  of cross-sectional area while the cylindrical scintillation detector, 5.0 inch in diameter  $\times$  4.0 inch height, would have about 125 times higher count rates.

The amount of Gd that reaches the tumor is approximately  $300 \mu\text{g/g}$  [12]. This is about one order of magnitude less than our detection limit. By increasing the source activity, two orders of magnitude or increasing the

detection efficiency two orders of magnitude, or both (four orders of magnitude) can increase the overall efficiency  $10^2$ – $10^4$  times. In this case, the detection limit can be much less than the actual Gd concentration in the brain. Additionally, one could consider a detector that accepts a wider angular dispersion of the fluorescence. The fluorescence is sufficiently well resolved from the Compton scattering, that using less collimation on the detector could increase the detected intensity without sacrificing discrimination.

The specific exposure rate constant for Am-241 is 0.0129 R/(h-Ci) at 1 m [13]. A 100 Ci Am-241 at 50 cm and 18 s exposure can be shown to give 0.026 R or approximately 26 mrad, or 0.26 mGy (0.26 mSv). While this value is larger than we prefer, it is less than the doses received in most general diagnostic examinations and much lower than the dose in fluoroscopy examinations.

The energy of 59.5 keV is quite suitable for this application. It is slightly above the 42.98 keV of Gd characteristics X-rays which make the probability of interaction high. At energy less than 50 keV, the interaction is not possible while at higher energy, the probability of interaction will decrease. One of the main advantages of Am-241 is its long half-life. In such a case, the source can be used for a very long time without affecting the sensitivity of the system.

X-rays from an X-ray machine could be used as a radiation source but the continuous spectrum of radiation will make analysis more difficult. For example, with a continuous incident X-ray spectrum, the scattered radiation peak coming from different components will be very wide. The Gd characteristic peak X-rays might not be resolvable. Moreover, the duration of exposure in most diagnostic X-ray generators is small; a fraction of a second.

As was mentioned earlier, MRI can also be considered to measure the concentration of Gd in brain tumors. To make this measurement, one must first measure the post contrast change in the T1 rate and then employ the T1 relaxivity R to determine the concentration. The value of R can be readily measured in aqueous solution, but in the brain the value is expected to be quite different. In a very recent publication, the T1 relaxivity R of Gd-DTPA was measured to be  $5.34 \text{ mM}^{-1} \text{ s}^{-1}$  in a 2.4 T field in a rat brain [14]. This value is considerably higher than previously estimated. Thus, the MRI remains qualitative until the relaxivity R is well-established; however, MRI is sensitive to lower concentrations of Gd than we could measure with X-ray fluorescence.

## Conclusions

The analysis of the X-ray fluorescence of Gd in brain tumors provides valuable information containing the

concentration of the Gd in the tumor. This can be used to calculate the effective dose to deliver to the tissue for maximal tumor destruction. The analysis consisted of variables that included the position of the head phantom; size of the tumor vessel, depth of the tumor vessel inside the head phantom and the amount of Gd in the tumor vessel. Using X-ray fluorescence proved to be better than trying to measure the optical density of X-ray images, where the measurements were not consistent for low Gd concentrations.

## References

1. Shih JL, Brugger RM (1992) Gadolinium as a neutron capture therapy agent. *Med Phys* 19(3):733–744
2. Harms AA, Norman GR (1972) The role of internal conversion electrons in gadolinium-exposure neutron imaging. *J Appl Phys* 43(7):3209–3212
3. Weinmann HJ, Brasch RC, Press WR, Wesbey GE (1984) Characteristics of gadolinium-DTPA complex: a potential NMR contrast agent. *Am J Roentgenol* 142:619–624
4. Allen BJ, McGregor BJ, Martin RF (1989) Neutron capture therapy with gadolinium-157. *Strahlenther onkol* 165:156–157
5. Miller GA, Hertel NE, Wehring BW, Hornton JL (1993) Gadolinium neutron capture therapy. *Nucl Technol* 103:320–331
6. Ichikawa H, Watanabe T, Tokumitsu H, Fukumori Y (2007) Formulation considerations of gadolinium lipid nanoemulsion for intravenous delivery to tumors in neutron-capture therapy. *Curr Drug Deliv* 4(2):131–140
7. Carlsson J, Forssell-Aronsson E, Glimelius B (2002) Radiation therapy through activation of stable nuclides. *Acta Oncologica* 41(7–8):629–634
8. Klykov SA, Ul'yanenko SE, Matusевич ES, Kurachenko YuA, Dulin VA (2004) Tissue absorbed dose from a gadolinium layer irradiated with neutrons. *At Energy* 96(6):430–433
9. Brugger RM, Shih JA (1989) Evaluation of Gadolinium-57 as a neutron capture therapy agent. *Strahlenther onkol* 165(2–3): 153–156
10. Yoshida K, Furuse M, Kaneoke Y, Saso K, Inao S, Motegi Y, Ichihara K, Izawa A (1989) Assessment of T1 time course changes and tissue blood ratios after Gd-DTPA administration in brain tumors. *Magn Reson Imaging* 7(1):9–15
11. Bartolini ME, Pekar J, Chettle DR, McNeill F, Scott A, Sykes J, Prato FS, Moran GR (2003) An investigation of the toxicity of gadolinium based MRI contrast agents using neutron activation analysis. *Magn Reson Imaging* 21(5):541–544
12. Shih JL, Brugger RM (1992) Gadolinium as a neutron capture therapy agent. In: Allen BJ, Moore DE, Harrington BV (eds) *Progress in neutron capture therapy for cancer*. Plenum Press, New York, pp 183–186
13. Shaper J (1981) *Radiation protection. A guide for scientists and physicians*, 2nd edn. Harvard University Press, Cambridge, p 232
14. Haar PJ, Broaddus WC, Chen ZJ, Fatouros PP, Gillies GT, Corwin FD (2010) Gd-DTPA T1 relaxivity in brain tissue obtained by convection-enhanced delivery, magnetic resonance imaging and emission spectroscopy. *Phys Med Biol* pp 3451–3465

Reproduced with permission of the copyright owner. Further reproduction prohibited without permission.